ABVR DEVELOPMENT FOR M&S PREDICTIVE IM TOOL

Jessica A. Stanfield and Jamie B. Neidert
Aviation and Missile Research, Development and Engineering Center, Redstone Arsenal, AL
Eric N. Harstad
Sandia National Laboratories, Albuquerque, NM
Bradley W. White and H. Keo Springer
Lawrence Livermore National Laboratory, Livermore, CA

EXECUTIVE SUMMARY

The U.S. Army Aviation and Missile Research, Development and Engineering Center (AMRDEC) developed and conducted a series of small scale fragment impact tests called Army Burn to Violent Reaction (ABVR). These test were focused on a High Performance Propellant (HPP), an Ammonium Perchlorate (AP), aluminum powder, and hydroxyl-terminated poly-butadiene binder formulation, in a 2-dimensional analog rocket motor configuration. These data has been used to enhance IM Hazards computer modeling & simulation (M&S) tools being developed primarily by the Department of Energy/National Nuclear Security Administration national labs. To validate the M&S tools, IM tests were also conducted using HPP in integrated analog demonstration rocket motors. The Joint Insensitive Munitions Technology Program (JIMTP) funded the test and demonstration efforts for some ABVR tests run in 2013 and for the analog demonstration tests. M&S efforts and some test diagnostics were supported by the Joint DoD/DOE Munitions Program (JMP). Both pre-test predictions and post-test M&S runs were conducted and the results were analyzed and compared with the test data.

INTRODUCTION

The work focused on small scale Fragment Impact (FI) testing. A Burn-to-Violent Reaction (BVR) Propellant Impact Test originally developed by Steven Finnegan at China Lake in the 1980s[1-3], was modified to create the Army- Burn to Violent Reaction (ABVR). This new test has been conducted at the U.S. Army Aviation and Missile Research, Development and Engineering Center (AMRDEC) on Redstone Arsenal in Huntsville, Alabama. The ABVR test was updated as a fragment impact sub-scale screening test to take advantage of current testing technologies, such as high speed digital video cameras[4-5]. In addition, three sub-scale integrated analog rocket motor tests were conducted to compare with the ABVR results and to evaluate the M&S tools.

The propellant composition explored in this program is a High Performance Propellant (HPP), which is composed of Ammonium Perchlorate (AP) and aluminum powder bonded by hydroxyl-terminated butadiene. The ABVR test set-up permits many variables to be explored including distance between propellant slabs, “case” materials, and projectile types and velocities. Blast gauges, high speed video, and analyses of remaining materials (energetic and inert) were employed to understand the reaction violence at differing velocities with differing impact threats.

The ABVR test was developed as a linear representation of an analog rocket motor, which allows visualization of the propellant behavior. This representation allows for multiple, inexpensive tests to be performed for guiding the FI predictive capability modeling efforts. The test article consists of two propellant samples placed on a stand with a gap between them representative of the central bore of a motor, see Figure 1. The samples have the candidate propellant (HPP) bonded to a case material or substrate. The test projectiles fired at the test article. The velocity of the projectile, high speed video, reaction residue, and the blast pressures are collected for post-test analysis.

ABVR tests were performed in approximately 7 sets of HPP testing from 2009 to 2013. Throughout the years of testing, many configurations were tested for a total of 79 tests. Examples include: plate spacing distances where the propellant changes from an endburner to a larger gap

with each test; a set test article configuration with varying impact velocities; one-sided test configurations, where the fragment impacted the plate, traveled through the propellant and impacted nothing on the other side; inert slab to propellant slab and vice versa; and some sphere projectile impacts that replicated specific fragment impacts. These tests were all done in an effort to better understand the violent reaction ignition point and determine outcomes after a threat has been introduced.

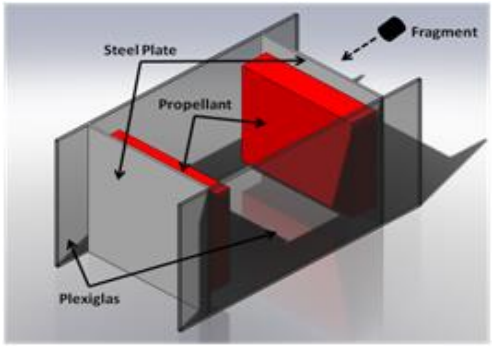

Figure 1. Standard Configuration ABVR Test

Data obtained from these ABVR tests, earlier (2009-10) Full Scale rocket motor IM tests, and material characterization testing was used in the enhancement of IM Hazards computer modeling & simulation (M&S) tools being developed by Lawrence Livermore National Laboratory (LLNL), Los Alamos National Laboratory (LANL), and Sandia National Laboratories (SNL). LLNL (see Springer et al.[6]) used a multi-physics, arbitrary-Lagrangian-Eulerian code (ALE3D) to simulate the ABVR tests with the Propellant Energetic Response to Mechanical Stimuli (PERMS) material model to explore reactivity. SNL used CTH[20], a multi-physics Eulerian shock hydrocode that utilized the PMOD[19] reactive flow model, which simulates the energetic response of Hazard Class 1.3 propellants under shock loading conditions, to model the ABVR tests. The characterization of the projectiles was done by LANL, and the subsequent material parameters were used by both ALE3D and CTH. Additional experiments were performed by LANL on the mechanical response of the propellants that were used in calibrating the models within the codes.

In 2013, following the ABVR testing with HPP, three integrated analog demonstration HPP rocket motors were tested under the fragment impact IM threat condition and considered to be the culmination of the previous tests (ABVR and Full Scale IM). The same DOE lab codes and models described above were used to predict the outcome of the tests.

EXPERIMENTAL & METHODS

ABVR Experimental Setup

ABVR tests were conducted at Redstone Arsenal, Aviation and Missile Research, Development and Engineering Center (AMRDEC) Test Area 10 site. The ABVR testing utilized the test area's projectile accelerator, pressure gauges, breakscreens and high speed cameras to create and record the events. The ABVR tests accelerated a saboted STANAG 4496 fragment or 440C stainless steel sphere out of a 20mm cannon. The STANAG fragment is cylindrical in shape with a conical tip. The fragment mass is 18.6gm, and is composed of a mild, carbon steel with HRB 100 (Hardness Rockwell B scale). The 5/8 in diameter sphere has a mass of 16.1 gm, and is composed of 440C stainless steel. The maximum velocity achievable in the test series was approximately 6000 ft/sec due to the limits of the 20mm cannon.

Series 1: Fragment projectiles were fired at 6in x 6in x 1/8in thick 4130 steel plates to learn characteristics of the impact interaction. The fragment was impacted at velocities ranging from 3000-6000ft/sec. The fragment or fragment pieces were collected in a Celotex bundle to analyze the deformation or breakup.

Four tests in the standard ABVR configuration were performed. The web thickness and air gap were chosen to represent the thinnest web and widest bore gap of the represented motor configuration. The fragment projectile impacted the test articles at targeted velocities of 3000, 4000, 5000, and 6000ft/sec to observe propellant breakup, formation of debris cloud inside the motor, and reaction. Pressure gauges were not used in this series. Pressure gauges

were introduced in series 2. A repeat of series 1 was conducted to gather more data on the varying reactions.

Series 2: Tests were conducted using a single live test article to analyze ignition of the damaged propellant and provide a better visual representation of the debris cloud formation. Previous testing demonstrated that ignition often occurs when the debris cloud from the first sample hits the second sample. Other experimental configurations in this series were set up to explore the source of ignition, post-impact projectile velocity, and projectile deformation.

Series 3: The tests were conducted at fragment velocities of 3000, 4000, 5000, and 6000 ft/sec. The air gap was 2.3 in for the fragment projectile tests and 6.1in for sphere projectile tests. Additionally four tests were conducted, in the standard configuration: two at 3000 ft/sec with a 2in and 4in air gap; and two at 6000 ft/sec with a 2in and 4in air gap. The goal was to determine if the sphere could cause more, equal, or less damage than the STANAG fragment and determine the response with the varied length of the air gap. Additional tests were conducted based on observations in series 2. The intention was to see if the fragment was leading the propellant debris or if the propellant was leading the fragment.

Series 4: This series continued testing to reduce the propellant debris cloud via a stripper plate at impact velocities between those previously studied. The tests conducted were intermediate of the previous tests.

Series 5: A test matrix was proposed with the intent to focus towards completing the 1.3 HPP propellant study. This matrix explores the variability in air gap and web thickness, and in steel-cased configurations. The steel case plates were held constant at 7 inch separation. See Figure 2 for images. Tests were also performed with no plate at varying velocities to see if the steel plate was a contributing factor to the reaction violence, or how the results would differ from similar tests with a steel plate.

Figure 2. Air Gap / Web Thickness Variability

Series 6: In this series, inert testing was revisited to capture open air pressure readings. In live propellant testing, low order reactions can produce peak pressures under 5psi. The goal of these inert tests was to determine if and how much of the pressure readings were attributed to the firing of the gun and impact of fragment or sphere on the steel plate. A couple of tests used aluminum plates for comparison. Inert propellant material was bonded to the plates and the test setup was in the standard configuration.

Series 7: This series would represent the analog motor in a 2-dimensional manner, including the shipping container used for storage. The composite plate material (rocket motor case) measured 6”x6”x1/8” and had 0.06” thick Kevlar-filled polyisoprene insulator adhered to it. The HPP slab was bonded to the insulator with a carbon filler/ Hydroxyl-Terminated Polybutadiene (HTPB) inhibitor approximately 0.03” thick. The HPP slabs measured 5in x5in x 3.65in, and had a 1.5inch air gap between the two slabs. See Figure 3.

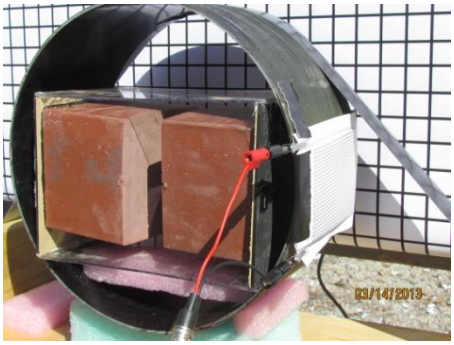

Figure 3. ABVR Representation of Analog Motor Tests

Analog Demonstration Rocket Motor

The analog demonstration rocket motor was designed to simulate a similar response to that of a full-scale motor. The test article was configured in a composite case cylinder measuring 9.1 inches in diameter and 18 inches in length, and was lined with HPP grain in a straight cylindrical configuration. The complete motor assembly was 27.86 inches in length. The case was 0.095 inch thick of Insensitive Munitions (IM)-7 Carbon/epoxy composite with S2 glass layers in the thicker aft closure joint. The case included a 0.06inch thick Kevlar-filled polyisoprene insulator and was fully lined with a carbon filler/HTPB inhibitor. The case contained approximately 65.4 lbs of propellant for the 2 inch bore configuration and approximately 54.3 lbs of propellant for the 4 inch bore configuration. The HPP was a Class 1.3C aluminized/HTPB propellant. The motor's case was designed for a Maximum Expected Operating Pressure (MEOP) of 3000 psi. See Figures 4 & 5 for details of the Analog Demonstration Rocket Motor. Three test articles were made; one had a 4 inch bore and two had a 2 inch bore. The test articles were subjected to fragment impact IM testing in accordance with MIL-STD-2105C. The IM tests were conducted to determine the event reaction type and analyze the IM Hazards model predictions of the HPP analog demonstration rocket motor when impacted with a STANAG fragment at one velocity, 8300ft/sec.

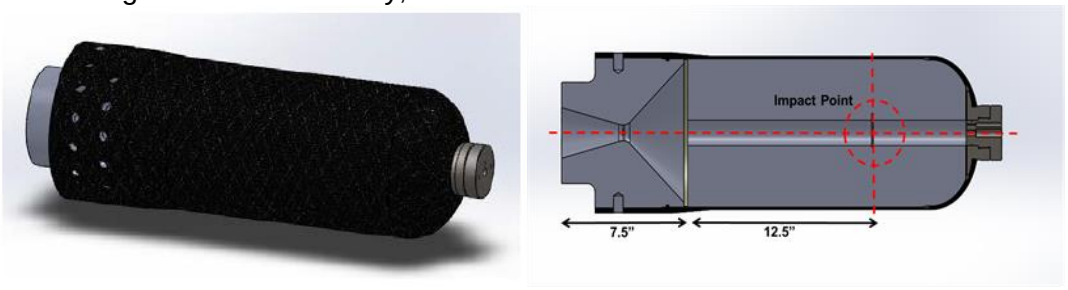

Figure 4 (Left). Analog Rocket Motor
Figure 5 (Right). Sectioned View of Analog Rocket Motor with Impact Point

Instrumentation for these tests included break screens to determine fragment velocity and time of fragment impact on the test article; open air pressure gauges located in the test field; high speed video cameras in three locations; Photonic Doppler Velocimetry (PDV) to determine case movement; a photodiode threaded in the test article nose to detect time of first light; and a piezoresistive pressure transducer threaded in the test article nose to detect in-bore pressure. A mirror was placed at approximately a 45º angle to provide orthogonal views, and a gauging system backdrop/grid board was emplaced behind the test item to determine the exact hit point of the fragment on the test article via high-speed photography.

M & S Methods

With the use of the earlier Full Scale Rocket Motor IM tests and the ABVR test data, the modelers made pre-test predictions for the analog demonstration rocket motor IM tests. These pre-test predictions helped define the test plan and test article design. Originally, the test article was designed to represent a rocket motor with a straight center-bore measuring 1.5 inches and a web of 3.65 inches. It was determined by the pre-test predictions and ABVR tests that the proposed test article dimensions might not allow for an adequate debris cloud to form thus reducing the violence, independent of the impact velocity. Canister, case, and insulation material were unexpectedly determined to reduce the impact velocity by approximately 15% in the pre-test M&S predictions. The test article design and test matrix were changed to address these findings.

LLNL utilized the ALE3D code with the PERMS reaction/burn model for this work. For ABVR simulations, Springer[7] describes, "2D-axisymmetric Eulerian calculations in ALE3D were

carried out with an outflow/pres-continuous boundary condition on the left-hand, top, and right-hand, sides of the simulation domain.

In 2013, LLNL conducted 'sensitivity studies on parameters used in the PERMS Equivalent Plastic Strain (EPS)-enhanced burning model parameters and their effects on the reactivity of the HPP to calibrate the model to ABVR tests and determine how these effects may inform full-scale rocket motor simulations that asses the response of the HPP due to high velocity fragment impact hazards'. See Springer[7]. After ABVR calculations were conducted, rocket motor 'analog simulations were performed to analyze the in-bore pressure, 90 degree case velocity, and time of first light due to propellant reaction.' 'Due to uncertainties in the HPP fragmentation response and its central role in capturing reaction violence we {LLNL} chose to vary the parameter A_0 in the PERMS EPS-enhanced burning equation to bound the hazard response violence. In addition to varying A_0, sensitivity studies were also carried out on the case strength, NATO fragment spall strength, and bore size to better understand their effects on case velocity and in-bore pressures.' See Springer[7]

SNL researchers utilized Version 10.3 of the Eulerian CTH shock physics code for this work All simulations utilized Adaptive Mesh Refinement (AMR), which allows for the simulation to be refined in areas of interest, and unrefined in other parts of the domain with the ability to refine based on user specified criteria. The materials in the simulations were modeled with the following: The cover plate and projectile were both modeled with the Zerilli-Armstrong Constitutive Model and Mie-Gruniesen equation of state. For the IM7 composite plate, either an elastic-perfectly-plastic model or the high fidelity Multi-constituent Composite Model (MCM) was used. The HPP was modeled using the reactive flow model PMOD (Propellant Model). PMOD was developed by SNL for 1.3 propellants and is a relatively simplistic model that does not include deviatoric strength of the propellant.

For the ABVR simulations, a 5m x 5m two dimensional cylindrical problem domain was used, which explicitly model the pressure gauges. The mesh size varied from 50cm x 50cm to 0.097656cm x 0.097656cm over ten levels of refinement. The AMR indicators were constructed to resolve the projectile and propellant local to the impact during the penetration, and to resolve the subsequent pressure wave that was created from the reaction. To recover the mass lost in the axisymmetric representation, the radius of the cylinder was increased slightly. The pressure data at the 8 gages was directly compared using tracer points in the simulations.

For Analog Demonstration Rocket Motor Test simulations, a three dimensional rectangular AMR problem domain X (-4m to 4m), Y (-1m to 7m), and Z (-4m to 4m) was used. A cubic mesh side varied from 100cm to 0.097656cm over ten levels of refinement. Even at this high resolution, it is extremely difficult to model the thin composite case and insulation layer. The simulations have approximately two cells across these parts and so SNL does not expect to accurately resolve the details of the case motion. Additional analysis has shown that there is significant case motion out of plane of the PDV gages, which are focused on a point in space that has material translating across it.

RESULTS

Baseline Pressure Reading: The peak pressures measured by blast gauges did not peak 1.5psi (range 1 meter). The tests used inert material to simulate the projectile-case interactions without introducing energetics. Pressure readings were used to baseline the energetic tests.
Projectile: The steel casing tests showed deformation of the fragment for an impact velocity of approximately 3000-4000ft/sec. As velocity increased, recovery of the fired projectiles became difficult due to the multiple fragments produced after impact. Dimensions were recorded and provided to modelers. This information was used as verification that the simulations were on track. Tests were performed to determine the responses from sphere and fragment projectiles. In Series 3, it was demonstrated that there was a significant difference in the reaction if the

projectile varied in geometry. Reaction violence was determined to be less violent at a known impact velocity when using a sphere. More tests would be required to identify the correlation.
Debris Cloud: The sequence shown below from Series 2, Figure 6, displays the density of the debris cloud as a function of velocity. These are four different tests with each at a different fragment velocity. One can see the debris cloud becoming less dense as the fragment velocity decreases. At 4000 and 3000 ft/sec the fragment can be seen leading the debris cloud.

Figure 6. Density of Debris Cloud as a Function of Fragment Velocity

In Series 3 and 4, the debris cloud was reduced so that the projectile could be seen, and a perpendicular inert surface for the propellant spall to strike was utilized. In these tests, the fragment was traveling at 3000 ft/sec with either a 2in gap or a 6in gap from the propellant surface to the debris stripper. The fragment was clearly visible once it passed through the debris stripper, and no ignition appears to have occurred in the high speed video upon propellant impacting the debris stripper. Although this was not seen in the video, the post test results suggest that there was a combustible reaction on the debris stripper for the 2 inch gap test. The 3000 ft/sec shot at a 6 inch air gap had no reaction. The debris stripper experiment was repeated at 6000 ft/sec which resulted in a violent reaction for both distances. The propellant spall ignited upon impacting the debris stripper.
Ignition Point: In Series 2 the Inert-Propellant test, the propellant surface was initially ignited when struck by the inert debris cloud. When the fragment and spall from inert material hit propellant, ignition was extinguished. The Propellant-Inert test experienced an ignition when struck by the live propellant. The combustion observed propagated back through the cloud transitioning into a violent reaction. This indicates that the debris cloud could be ignited from striking a perpendicular surface.

Shots were performed at 3000 and 6000 ft/sec with a single slab of propellant. The fragment first impacts the steel plate and follows through to the propellant. Neither shot ignited at any point in time, but they did display the amount of damage done to the propellant as a function of fragment velocity. This demonstrates that the higher the velocity (energy) the greater the quantity of propellant spalls.

Case Material: The HPP test series with no steel plates resulted in significantly reduced reactions. It is evident the rigid case material increases the shock locality imparted onto the propellant sample thus creating more damage to the first propellant slab.
ABVR Test Result Summary: See Figure 7. The CPPC test produced a reaction violence registering 56psi. When the configuration changed to CPIC, reaction peak pressure decreased to 41psi. The CPPC and CPIC test appeared to have the majority of the propellant react. These tests show the start of reaction to occur as the debris cloud impacts the second slab of material. In the CIPC test, reaction violence significantly drops off to approximately 8psi. In the high speed videos pertaining to test CIPC, no ignition is even observed. The NPPN test had a comparable pressure reading (7psi) to CIPC, but ignition and a continued combusting reaction was observed after the debris cloud impacted the second slab. The CIIC tests were performed to provide data on an inert test to compare low order reactions or no reaction tests.

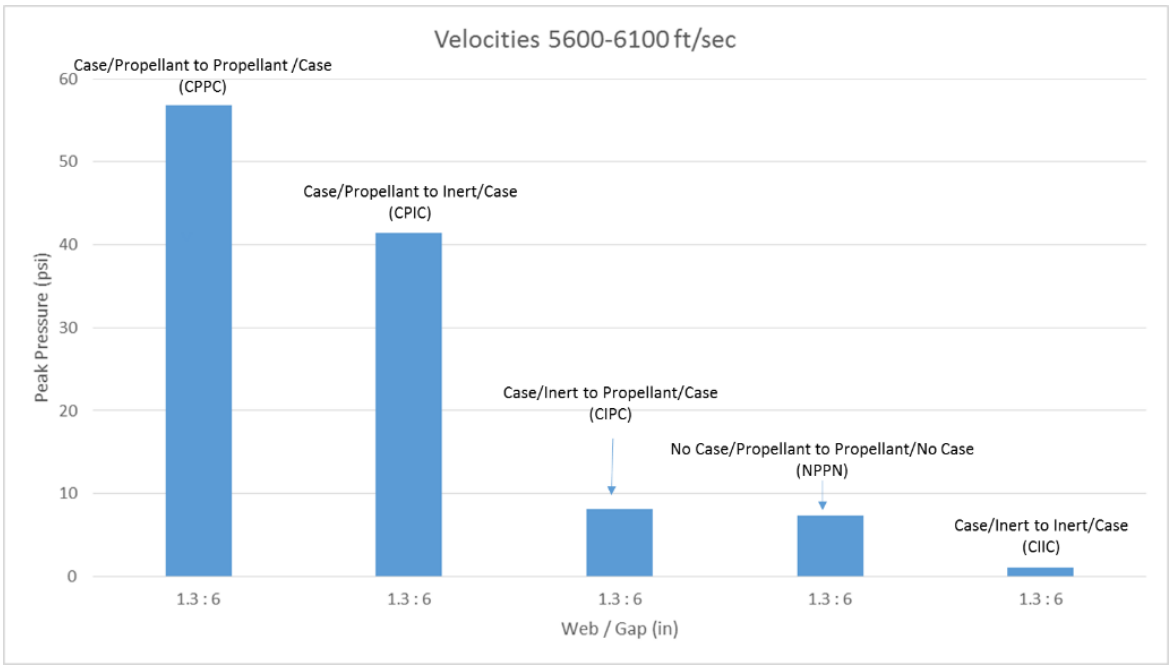

Figure 7. ABVR Tests: Similar Velocity, Web and Gap; Variations in Case and Propellant.

Figure 8 is a representation of the violence that occurred at the varied web thicknesses and air gaps with similar velocities. It is apparent that changing the dimensional material path the fragment travels through effects the outcome of the reaction.

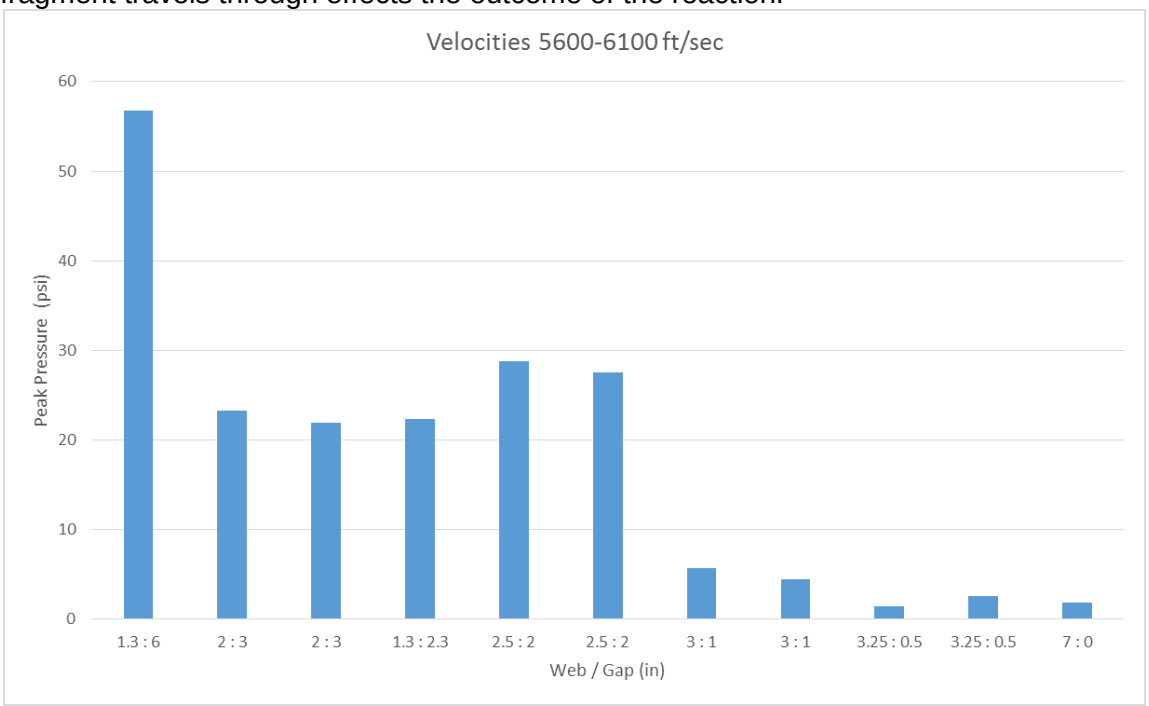

Figure 8. ABVR Tests with Similar Velocity and Various Web and Gap

Series 7 ABVR tests demonstrated a significant reduction in impact velocity due to the presence of the canister, composite case, and insulation material. The percentage velocity reduction can be seen in Table 1, Tests 1-4.

Table 1. HPP ABVR Series 7 Test Results

Test Number	Canister	Composite Panel	Insulation	Test Article	Velocity, ft/sec	% Velocity Reduction	Reaction Type	Peak Pressure, psi
1	X				6211	7	None	N/A
2		X			6374	5	None	N/A
3		X	X		6250	8	None	N/A
4	X	X			6179	15	None	N/A
5	X			X	6237	N/A	Burn	11
6				X	6217	N/A	Burn	26
7				X	5177	N/A	Burn	15
8				X	3993	N/A	Burn	4.5

The composite material and adhered-insulator proved to reduce the impact velocity more than anticipated (approximately 8%), and the fragment speed reduction due to the canister with a composite plate at a 1.5 inch stand-off had a surprising 15% reduction in velocity . The violence of the reaction increased with fragment impact speeds as expected in the tests with no canister. The test (#5) that included the canister was intended to have a fragment impact at approximately 6200ft/sec on the test article, but the impact velocity on the test article was reduced to approximately 5800ft/sec due to the canister. This resulted in decreased pressure, which has been related to a decrease in violence. What would have likely had a peak open air pressure of about 26psi was reduced to about 15psi by adding the canister. These findings were valuable for the modeling efforts.

Analog Demonstration Rocket Motor Test Results

Analog demonstration tests, were impacted with the fragment at the intended impact aim point. The data recorded during the three tests is summarized in Table 2. The maximum over pressure (OP) is split into two sections for the four stems of pressure gauges. Stems 1 and 4 were located on the impacted side of the test article, and Stems 2 and 3 were located on the opposite side of the impacted test article. The separation of the pressure gauges helps track the direction of the reaction. In general, higher pressures were seen on the impacted side of the test article in Tests 1 and 3, whereas Test 2 had a more equivalent pressure reading on both sides. This suggests the reaction was more violent in Test 2.

In-bore pressure readings suggest that the canister reduced the violence of the reaction. Tests 1 and 2 did not capture the peak reading due to the limited capacity of the gauge (10K psi), but it did record Test 3 at 8400psi before the data exceeded the rating of the gauge. The in-bore pressure gauges on all three tests recorded values indicating their rated capacity was exceeded; therefore data is suspect after the gauge rating was exceeded.

The case velocity after impact, as measured by PDV, was recorded at two different angles (90 and 135 deg.) from the impact point on the rocket motor case. The second test did not record PDV data due to a data acquisition error. Test 1 recorded velocities greater than Test 3, which may be attributed to the addition of the canister in Test 3. In both tests, the velocities reported here are the maximums in the first peak of PDV data.

Unfortunately, photodiode data was only recorded in Test 3, which showed first light to occur 213 µsec after fragment impact with the test article.

Unofficial assessment is that these were Reaction type IV. Debris locations were mapped in addition to instrumented results to assist in the determination of reaction type.

Table 2. Summary of IM Analog Demonstration Rocket Motor Test Data

Test	Velocity, ft/s	Max OP 5ft, psi	In-Bore Pressure, (psi)	Reaction Type
1	7989	12	>10K	IV
2	8399	20	>10K	IV
3	8279	11	8400	IV

M & S Comparisons to Data

CTH and ALE3D pre-test predictions were conducted prior to analog test. Posttest continued iterations of the simulations were conducted to improve the models' response to these complex scenarios and to adjust for the actual experimental conditions; see Table 3 for final results. Note, grey font used in Table 3 distinguishes values requiring further explanation in following paragraph.

The PDV data points in the summary table are the maximums of the first peak of the data. The M&S case velocity values were obtain by observing the velocity of the initial aim point moving in the direction of the respective gauges consistently higher than these data points, and in general, all of the PDV data. A possible explanation for this is the case is the case is translating in directions oblique to the PDV gauges and so they are recording velocities that are not associated with the same location on the case. We have demonstrated this through M&S, but have not determined how to directly compare with the experimental data.

The photodiode data for Test 3 results indicate the codes are reasonably accurate in predicting the time to first light inside the rocket motor analog. First light was determined from the simulations as the time when the fragment reached the far side of the bore.

For the overpressure gauge results, further work is needed on ALE3D to capture the longer time frames needed to model the blast wave at relatively long distances away from the impact article. From the CTH results, the simulations show slightly higher pressures than indicated in the data, but it appears the physics of the blast waves are being reasonably well modeled in Tests 1 and 2.

Issues with the rating of the in-bore pressure gauges have been discussed above. In general, the M&S results show reasonable agreement with the data that is available.

Table 3. Post Test Simulations Compared to Test Data (ranges in calculations are based on propagating propellant characterization data uncertainties through model parameters)

Data Type	Case Velocity (PDV 90° probe), ft/s	Photodiode, µsec	Max. OP, psi	In-bore pressure, psi	Penetration through Test Article
Raw Test 1	43	No Data	12 at 5ft 5 at 10ft	>10K	No
CTH Test 1	140	N/A	16 at 5ft	40K	No
ALE3D Test 1	170-210	85-90	N/A	8-19K	No
Raw Test 2	No Data	No Data	20 at 5ft 9 at 10ft	>10K	Unknown
CTH Test 2	100	N/A	32 at 5ft	13.5K	Yes
ALE3D Test 2	295	102	N/A	13.6K	Yes
Raw Test 3	7.5	213	11 at 5ft 5 at 10ft	8400	Unknown
CTH Test 3	75	260	N/A	6700	No
ALE3D Test 3	280	165	N/A	6000	No

CONCLUSIONS

The Army Burn-to-Violent test has been demonstrated to be effective in characterizing the IM hazards of fragment impact for both standard STANAG fragments and spheres using High Performance Propellant (HPP). The ABVR test procedures developed in this project characterized major parameters including projectile composition, fragment velocity, and test article configurations for the purpose of modeling predictions.

Reaction violence for the ABVR test with HPP proved difficult to quantify as the propellant is not an ideal explosive or a 1.1 propellant (detonable). Violence was best determined through observation and pressure readings, but there is not a set boundary condition that strictly identifies each test's outcome. Tests were identified as more, less, or equivalently violent to each other based of the test data results

Significant reaction variance was recorded with the different test configurations; the impression is that the breakup size of the propellant particles, debris cloud speed, and shock impedance from the case all contribute to the reaction violence. The HPP tests with no steel plate verified that steel plates add a significant increase to the reactivity of the experiments. Changing the dimensions (web and propellant thickness) of the path the fragment travels through affects the outcome of the reaction as well. This has been shown to be based on the size, density, and velocity of the debris cloud created as it travels across the air gap.

The analog demonstrations tests were judged to be IM Reaction Type IV for all analog motor designs; with and without canister, and the varying bore sizes. The canister appeared to mitigate the reaction of the motor due to fragment impact based on visual inspection and lower pressure readings. It is uncertain if the canister had been confined whether it would have created more damage or not.

The refined post-test ALE3D and CTH simulations provided values that were improvements to the original predictions. Due to the gaps in the test data and needed improvements in the M&S technology noted above, further experimental work and modeling enhancements are needed to continue to evolve predictive capabilities in the future. Post-test simulations also showed that it is helpful to quantify uncertainties in characterization data and propagate those uncertainties through model parameters to develop bounding calculations.

ACKNOWLEDGEMENTS

The authors would like to recognize Joey Reed, William Delaney, Brian Curtis, Zachary Hoernschemeyer and David Huebner for their support in performing experiments. This work was performed through support of the Joint Insensitive Munitions Technology Program and the Joint DoD/DOE Munitions Program.

REFERENCES

1. Finnegan, S.A., Pringle, J.K., Atwood, A.I., Heimdahl, O.E.R., and Covino, J., *Characterization of Impact-induced Violet Reaction Behavior in Solid Rocket Motors Using a Planar Motor Test Model*, International Journal of Impact Engineering, Vol. 17, pp. 311 – 322, 1995.
2. Finnegan, S.A., Atwood, A.I., Pringle, J.K., Zwierzchowski, N. G., Curran, P.O., and Wiknich, J., The Application of Ballistic Impact and Radiant Ignition Techniques for Characterization of Violent Reaction in Cased Propellant, Proc. 10th International Detonation Symposium, ONR 33395-12, pp. 320 – 339, 1993.
3. Finnegan, S.A., Heimdahl, O.E.R., Atwood, A.I., Pringle, J.K., Overview of Burn-to-Violent Reaction (BVR) Propellant Impact Test, Naval Air Warfare Center, Weapons Division, China Lake, CA 93555 Report No. NAWCWD TP 8691, September 2009.
4. Stanfield, J.A., Chew, W.M., Neidert, J.B., Johns, P., Huebner, D., and Reed, J.M., *Development and Validation of Army Modified Burn to Violent Reaction (ABVR) Testing*, Proc. 2009 JANNAF Propulsion Systems Hazards subcommittee Meeting, JSC CD-60, December 2009.
5. Stanfield, J.A, Chew, W. M., Johns, P.S., and Reed, J. M., *Army Burn-to-Violent Reaction (ABVR) Test Update: A Sub-Scale IM Screening Test,* 36th PEDCS 2010 JANNAF
6. Springer, H.K, Leininger, L.D., Nichols III, A.L., Reaugh, J.E., Stanfield, J.A., Neidert, J.B., *Benchmarking ALE3D Modeling with Army Burn-to-Violent Reaction(ABVR) Sub-Scale Rocket Motor Impact Experiments,* LLNL-TR-648487. Lawrence Livermore National Laboratory, Livermore, CA.
7. Springer, H.K. and White, B.W. INSENSITIVE MUNITIONS AND SURETY PROJECT ANALOG ROCKET MOTOR CALCULATION-Modeling the Fragmentation Impact Hazard Response of HPP during ABVR and Full-Scale Rocket Motor Analog Tests, FY2013 Draft

TCG-III: Energetic Materials Annual Report, Lawrence Livermore National Laboratory, Livermore, CA.
8. High Performance Propellant (HPP) Experimental Characterization, LA-CP-12-00953, C. Liu, C. M. Cady, et. al., 31 July 2012.
9. High Performance Propellant (HPP) Experimental Characterization, LA-CP-13-00953, C. Liu, C. M. Cady, et. al., July 31, 2012
10. *High-Performance Propellant Impact Test Report,* LA-CP-13-01468, M. J. Marr-Lyon, T. D. Sandoval, D. H. Herrera, J. A. Heidemann, 12 November 2013
11. *Sub-Scale Rocket Motor Impact Experiments*, H. K. Springer, L. D. Leininger, 2013 LANL paper published in the JANNAF proceedings
12. Overview of Burn-to-Violent Reaction (BVR) Propellant Impact Test, S. A. Finnegan, et. al., NAWC/AMRDEC-0514, October 2009
13. Experimental and Theoretical Investigations On Epoxy 55a Resin and Graphite-Epoxy 55a Composites, B. E. Clements, et. al., LA-UR-12-00638, January 3, 2012